

Levee Effect and Urban Development under Climate Change: Land-Use Strategies for Managing Residual Flood Risk in Taiwan

Hsueh-Sheng Chang, Chih-Po Hsu

(Prof. Hsueh-Sheng Chang, National Cheng Kung University, Department of Urban Planning, Tainan, Taiwan, changhs@mail.ncku.edu.tw)

(Chih-Po Hsu, National Cheng Kung University, Department of Urban Planning, Tainan, Taiwan, tommyuk55@gmail.com)

1 ABSTRACT

Urban flooding has become an increasingly severe challenge due to rapid urbanization and climate change, particularly in regions like Taiwan. The combination of steep rivers, mountainous terrain, and frequent typhoons heightens the risk of flooding. Traditional flood control measures, such as levees and drainage systems, have provided protection, but they have also led to unintended consequences. One notable consequence is the Levee Effect, where flood protection infrastructure encourages urban expansion into flood-prone areas, ultimately increasing long-term exposure to extreme flood events. This issue underscores the importance of addressing Residual Flood Risk, which remains even with existing flood control measures, especially regarding land-use dynamics. In this study, we integrated CA-Markov and SOBEK 1D-2D models to evaluate land-use changes and flood risk under different levee heights (6 meters and 10 meters) in Wugu District, Taiwan. Preliminary results indicate that land-use change is closely linked to flood inundation. While flood protection measures reduce inundation areas, urban expansion driven by these measures can still lead to increased flood risk under extreme rainfall events due to changes in land use patterns. In the event of a 650 mm rainfall over 24 hours, unrestricted development significantly raised flood risk and potential economic damages. Conversely, imposing development restrictions effectively reduced potential damages. These findings emphasize the necessity of land-use controls in managing residual flood risk. While levees can lessen flooding under typical conditions, they also promote land development that increases vulnerability to extreme events. This study highlights the need for a hybrid flood risk management strategy that balances structural defences with spatial planning and adaptive policies to improve climate resilience and support sustainable urban development.

Keywords: levee effect, residual flood risk, land use management, CA-Markov, SOBEK model

2 INTRODUCTION

Urban flooding has become a significant challenge in the 21st century, primarily driven by rapid urbanization and climate change (Merz et al., 2021; O'Donnell & Thorne, 2020). Taiwan, characterized by steep rivers, mountainous terrain, and frequent typhoons, is particularly vulnerable to flood disasters. Traditionally, flood risk management has relied on structural interventions such as levees, embankments, and drainage systems (L. Wang et al., 2022). However, the increase of impervious surfaces due to urbanization has worsened stormwater runoff, while climate change has intensified extreme precipitation events, often surpassing existing flood protection standards (Davenport et al., 2021; Li et al., 2024). These factors highlight the limitations of conventional flood control methods in addressing evolving flood risks (Butcher et al., 2023; Kim et al., 2023).

Additionally, the paradoxical relationship between land development and flood risk, known as the Levee Effect, poses a major challenge in flood-prone areas (Fusinato et al., 2024; White, 1958). Research indicates that flood control infrastructure can create a false sense of security, leading to accelerated urban expansion in floodplains and increased exposure to flood hazards (Di Baldassarre et al., 2018; White et al., 2001). When rainfall exceeds the protection threshold, the consequences can be devastating, resulting in significant socioeconomic losses (D'Angelo et al., 2020; Ferdous et al., 2019; Ludy & Kondolf, 2012). This Levee Effect perpetuates a cycle in which flood protection measures encourage more land development, inadvertently increasing long-term flood risk (Ding et al., 2023; Ferdous et al., 2019).

As illustrated in Fig. 1, this cycle can be worsened by climate change and urban expansion. The figure shows that flood protection standards reduce damage within their design thresholds, but residual flood risk persists when rainfall exceeds these standards (Roberto et al., 2015). Moreover, changes in land use after the construction of flood defences can significantly elevate flood exposure and potential damage (Breen et al., 2024). Unregulated urban development, coupled with intensifying precipitation, can create a dangerous

feedback loop in which rising flood risks necessitate additional structural interventions, ultimately exacerbating long-term vulnerabilities.

In light of these challenges, recent discussions in flood risk management have underscored the importance of Residual Flood Risk – the risk that remains despite protective measures (Serra-Llobet et al., 2022). Existing studies have primarily focused on rainfall events that exceed design standards, often overlooking the impact of post-construction land-use changes that further increase flood risks. The Intergovernmental Panel on Climate Change (IPCC) Sixth Assessment Report (AR6) emphasizes the need to integrate both structural and non-structural flood mitigation strategies, particularly focusing on spatial planning as a means to manage flood risks effectively.

Given these considerations, this study aimed to explore how spatial planning and land-use management strategies can effectively mitigate residual flood risk in rapidly urbanizing flood-prone regions. To achieve this, we employed the CA-Markov model to simulate future land-use scenarios and analyze the impact of urban development on flood exposure. The study incorporated flood inundation models to assess changes in flood risk before and after levee heightening. Additionally, we evaluated the effectiveness of various land-use management strategies, including floodplain zoning, low-impact development (LID) measures, and green infrastructure, under climate change-induced extreme precipitation scenarios. Through flood risk assessment with the estimated direct flood damage, this research aimed to establish a framework that balances urban development with effective flood risk management, ultimately contributing to resilient urban planning in the face of climate change. This study provided empirical insights into the interaction between land-use policies and flood risk dynamics, offering valuable guidance for policymakers in developing adaptive, risk-informed spatial planning strategies.

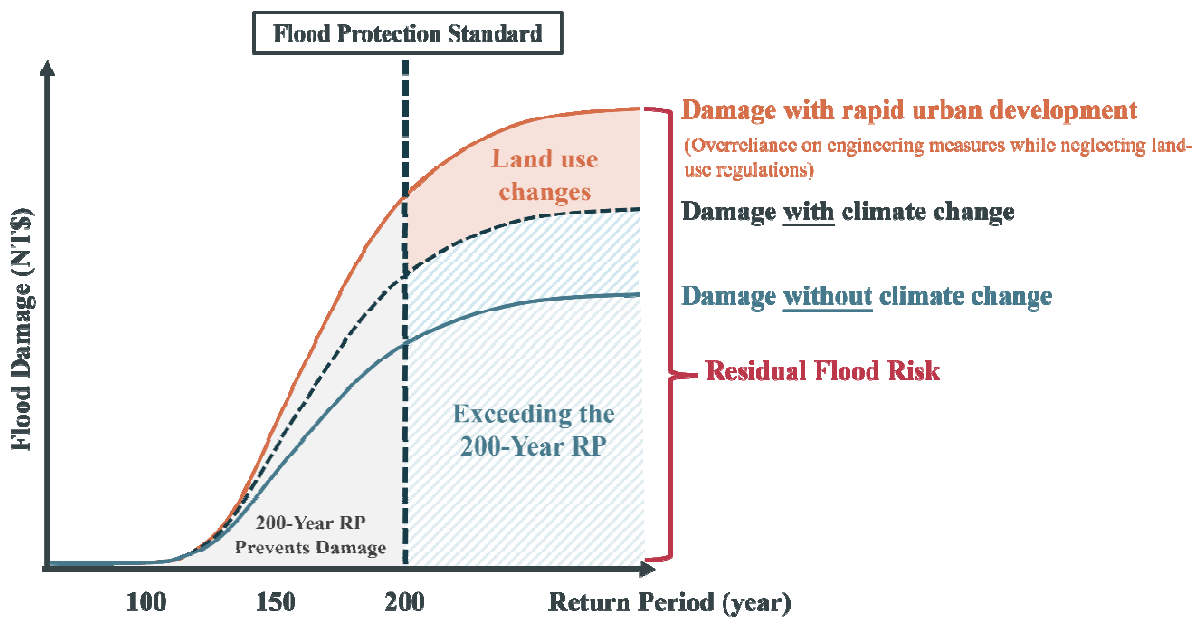


Fig. 1: Impacts of Land Use Changes and Climate Change on Residual Flood Risk Beyond Structural Protection Measures. Modified from Tanoue et al. (2021)

3 METHODOLOGY

3.1 Research Framework

This study combined flood risk management with urban development planning by analyzing the effects of flood inundation and structural flood control measures on land-use changes. The research framework consisted of four main phases: (1) simulating land-use changes using the CA-Markov model, (2) modeling floods with the SOBEK 1D-2D coupled model, (3) developing land-use management strategies for different scenarios, and (4) assessing flood risk through direct flood damage analysis. This integrated approach allowed for a comprehensive evaluation of residual flood risk and the effectiveness of land-use strategies in reducing flood risk. The first phase utilized the CA-Markov model to simulate land-use changes under 6M and 10M levee conditions, incorporating flood inundation data as a key driver. The second phase applied the SOBEK 1D-2D model to simulate flood inundation across various return periods (10, 25, 50, 100, and 200

years) for both 6M and 10M levees. The third phase assessed land-use management strategies for residual flood risk mitigation, examining six scenarios: business-as-usual (BAU), flood risk regulations, Low-Impact Development (LID), Green Infrastructure (GI), and integrated strategies. The final phase conducted a flood risk assessment, estimating flood direct economic losses across residential, commercial, industrial, and agricultural areas. This study aimed to explore the impact of land-use management strategies on residual flood risk in the context of the levee effect and climate change.

3.2 Study Area

This study focused on Wugu District in New Taipei City, Taiwan, as shown in Fig. 2. Its low-lying terrain and poor drainage make it highly susceptible to flooding during typhoons and heavy rainfall. Currently, the levee height is 6 meters, protecting for a 20-year return period, which is inadequate for extreme hydrological events. Plans are in place to raise the levee to 10 feet (3.05 meters) to meet the 200-year return period standard, aligning with the Greater Taipei Flood Control Plan. Land use in Wugu is regulated by the Tamsui River Floodplain Control Regulations, requiring municipal approval for construction and modifications. Future development will focus on the Wugu New Town Comprehensive Development Plan to enhance land value and urban growth. This study assessed how the levee height enhancement impacts land use and flood risk under various management scenarios, providing insights for improved flood control strategies and sustainable urban planning in Wugu.

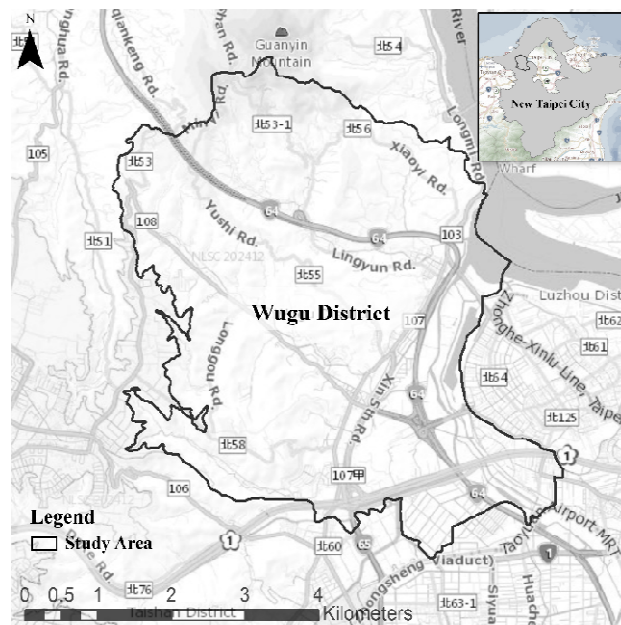


Fig. 2: Location of study area.

3.3 Land Use Change Simulation with CA-Markov Model

3.3.1 Overview of CA-Markov model

This study aimed to examine the relationship between changes in flood inundation areas and future land use transitions after the implementation of structural flood control measures. We used the CA-Markov model, which integrates the Markov Chain (MC) model and the Cellular Automata (CA) model, to simulate future land use changes. This model has been widely applied and validated in urban growth modeling and land use change analysis for its accurate and realistic results (Chakraborty et al., 2022; Tan et al., 2024). The MC model estimates land use transition probabilities based on historical trends, generating a Transition Probability Matrix to predict the likelihood of land conversion between different land use categories in the target year (S. Wang & Zheng, 2023). However, the MC model only qualifies changes between land use types and does not account for spatial variations (Moghadam & Helbich, 2013). Given this, the CA model, which has been widely applied in Spatially Explicit Models (SEMs) to capture the dynamics of geographical phenomena such as land use changes (Tong & Feng, 2020), was combined with the MC model. The CA model operates on a cell-based structure, where each cell's future state is determined by neighborhood effects and a local transfer function based on the current state of adjacent cells (Al-sharif & Pradhan, 2014;

Chakraborty et al., 2022; Liu & Feng, 2012). Additionally, this study built on the work of Lu et al., (2018) and Wang & Zheng (2023) by integrating Multi-Criteria Evaluation (MCE) to generate suitability maps for different land use types, incorporating key environmental and socioeconomic factors along with spatial constraints. We integrated the CA-Markov model with MCE to provide a comprehensive approach to land use simulation, incorporating flood inundation areas as a key factor in land use changes and urban development.

The structure of the CA-Markov model included four phases. In Phase 1, the MC model was first applied to calculate land use transition probabilities based on historical land use data. The 1995 and 2015 land use maps are classified and standardized into a grid-based format, forming the basis for computing the Transition Probability Matrix (TPM). In Phase 2, the study integrated driving and constraint factors into a MCE framework to generate suitability maps that refine spatial land use allocation. First, a review of previous studies informs the selection of environmental and socioeconomic factors, which are standardized using fuzzy membership functions to ensure comparability across variables. Cramer's V correlation coefficient was then used to measure the association between each factor and land use transitions. The Weighted Linear Combination (WLC) method is applied to systematically determine factor weights, avoiding subjective assignments. The resulting MCE-WLC model produces suitability maps for all land use categories, guiding the spatial distribution of land use changes. In Phase 3, the CA-Markov model integrates transition probabilities from the MC model with suitability maps from MCE, allowing for spatially explicit land use simulation. To assess model accuracy, the study simulates the 2021 land use map and compares it with observed data. Kappa Index statistics (including K_{standard}, K_{no}, K_{location}, and K_{locationStrata}) are used to evaluate the model's agreement with real-world land use distributions. If the validation results demonstrate high consistency, the model proceeds to predict the 2035 land use scenario.

3.3.2 Data Collection and Preprocessing

The CA-Markov model required multiple datasets, including land use maps, driving factors, and constraint factors (e.g., Digital Terrain Model (DTM), population density, and flood inundation areas). In this study, we utilized 1995 and 2015 land use maps from the National Land Surveying and Mapping Center of Taiwan to simulate future land use changes, while the 2021 land use map was used to validate the projected 2021 land use scenario. The original land use maps contained approximately 50 land use categories, with classifications varying across different years. To ensure consistency in analysis, we reclassified the 1995, 2015, and 2021 LULC maps into 11 standardized categories: agricultural land, forest land, transportation land, water bodies, commercial land, residential land, industrial land, green space, recreational land, vacant land, and other land uses. Since the TerrSet model operates exclusively on raster data, all LULC maps were converted from vector to raster format, with a spatial resolution of 10 × 10 m grid cells. Additionally, most driving factors were derived from the 2015 LULC map, except for DTM, slope, land with slope greater than 30%, population density, and flood inundation areas, which were obtained from separate datasets. Notably, this study incorporated flood inundation maps under different rainfall scenarios, produced by the Water Resources Agency (MOEA) in Taiwan, as a crucial factor influencing future land use changes.

3.3.3 Markov Chain (MC) Model

The MC model is a stochastic process model that describes the probability of a state transitioning into another (Jokar Arsanjani et al., 2013). In LULC analysis, the MC model quantifies transition rates between different land use types and has been widely applied in spatial forecasting (Sang et al., 2011). Since the MC model assumes that future transitions depend solely on the current state, it is particularly effective in predicting LULC changes under stable policy conditions, where past trends provide a basis for estimating future transitions (Wang & Zheng, 2023). The model employs a transition probability matrix to determine the likelihood of one land use type changing into another over a specified period (Lu et al., 2018). However, as the MC model does not incorporate spatial distribution patterns, it is often integrated with the CA model to improve spatial accuracy and predictive performance (Aburas et al., 2016; Adnan et al., 2020). LULC changes within the MC framework are predicted using the following equation (Adnan et al., 2020; Sang et al., 2011):

$$S(t + 1) = P_{ij} \times S(t) \quad (1)$$

where $S(t)$ and $S(t+1)$ represent the system status at time t and $t+1$, respectively; the transition probability matrix P_{ij} is defined as follow:

$$P_{ij} = \begin{bmatrix} P_{11} & P_{12} & \dots & P_{1n} \\ P_{21} & P_{22} & \dots & P_{2n} \\ \dots & \dots & \dots & \dots \\ P_{n1} & P_{n2} & \dots & P_{nn} \end{bmatrix} \quad (2)$$

$$\left(0 \leq P_{ij} < 1 \text{ and } \sum_{j=1}^n P_{ij} = 1, (i, j = 1, 2, 3, \dots, n) \right)$$

where P_{ij} represents the likelihood of transitioning from status i to status j ; n refers to the total number of land use categories. In this study, the transition probability matrix was derived from LULC changes observed between 1995 and 2015 to predict the 2021 LULC map for validation and the 2035 LULC map as the target projection.

3.3.4 Cellular Automata (CA) Model

The CA model is a cell-based simulation approach that captures spatiotemporal dynamics through local interactions, where each cell's future state is influenced by adjacent cell states and governed by predefined transition rules (Chakraborty et al., 2022; Lu et al., 2018). This model has been widely applied in land-use change and urban dynamics studies and has been integrated into various simulation tools, including CA-Markov in IDRISI, UrbanSim, and SLEUTH (Tong & Feng, 2020). The CA model consists of four key components, formally expressed as Eq. (3): lattice (L), state space (Q), neighborhood template (δ), and local transition function (f) (Adamatzky, 2018). When combined with the Markov Chain (MC) model, the CA-Markov model enables cells to transition independently based on neighbourhood transition rules and assigned transition probabilities, enhancing spatial continuity and predictive accuracy.

$$A = [L, Q, \delta, f] \quad (3)$$

3.3.5 Driving and constraint factors for land use changes

Land use changes are driven by a combination of environmental, socioeconomic, and policy-related factors (Dewan & Yamaguchi, 2009). The integration of Markov Chain (MC) and Cellular Automata (CA) models provides a robust framework for incorporating both environmental and socioeconomic variables, while simultaneously considering various spatial factors for simulating land use changes (Adnan et al., 2020). Environmental factors, such as topography and amenities, determine land suitability, with flat terrain facilitating development (Aburas et al., 2016). Socioeconomic factors, including population density and real estate values, are essential drivers of urban densification (Chakraborty et al., 2022). Similarly, built environment and infrastructure factors, such as accessibility to roads and highways, establish the connection between development causes (e.g., transportation networks) and their subsequent effects (e.g., urbanization) (Aburas et al., 2016). Furthermore, flood risk variability has been identified as a critical determinant of land use patterns, as areas subject to frequent flooding often undergo land use transitions. Research on the levee effect suggests that flood engineering structures can effectively reduce flood inundation areas, subsequently altering land development trends (Lu et al., 2018). Given this dynamic relationship, this study incorporates flood inundation areas as a key factor to examine the interactions between flood extent changes and land use transitions, thereby contributing to a better understanding of flood risk dynamics.

Cramer's V values were also employed to assess driving factors' significance and explanatory power in predicting future land use changes. A higher Cramer's V value signifies stronger explanatory strength, indicating that the corresponding variable plays a more substantial role in LULC change projections (Islam et al., 2018; Sisay et al., 2023). This study selects driving and constraint factors based on previous literature and their relevance to land use change modeling within the CA-Markov framework. As shown in Table 1, the

driving factors encompass environmental variables, including DTM, slope, proximity to rivers, and flood inundation areas, which influence land suitability based on physical geography and hydrological conditions. Socioeconomic and built factors include population density and proximity to public facilities, roads, residential, commercial, and industrial areas, reflecting the impact of accessibility and urban infrastructure on land use patterns.

For constraint factors, this study considers transportation land, forest land, water bodies, and areas with slopes greater than 30%, as these regions have limited transformation potential in real-world scenarios, thereby enhancing the accuracy of land use change modeling. To further explore the relationship between flood inundation areas and land use changes, this study initially utilizes flood inundation maps under four different rainfall scenarios, provided by the Water Resources Agency (MOEA), Taiwan. Subsequently, the SOBEK model is employed to simulate flooded areas under varying return periods, providing a more comprehensive understanding of flood impact on land use transitions.

Driving Factors		Constraint Factors
Environmental Factors	Socioeconomic and Built Factors	
DTM	Population density	Transportation land
Slope	Distance to public facilities	Forest land
Distance to river	Distance to roads	Water bodies
Flood inundation areas	Distance to residential areas	Land with a slope greater than 30%
N/A	Distance to commercial areas	N/A
N/A	Distance to industrial areas	N/A

Table 1: Driving factors (environmental, socioeconomic, and built) and constraint factors selected in the CA-Markov model

3.3.6 Fuzzy membership for driving factors and Boolean values for constraint factors

This study employed fuzzy membership functions and Boolean values to evaluate land suitability based on various driving and constraint factors. Constraint factors were assigned Boolean values (0 or 1) to restrict land use transitions, while driving factors were standardized using different fuzzy membership functions, including linear, sigmoidal, and J-shaped functions – based on their characteristics to assess the suitability of land use variations (Lu et al., 2018). The fuzzy membership function quantifies the degree to which a data point belongs to a fuzzy set, with values ranging from 0 to 1 or 0 to 255 (Bianchini et al., 2019).

As illustrated in Fig. 3, distance-related driving factors (e.g., proximity to roads and public facilities) were standardized using the Sigmoidal membership function with an S-shaped curve, where suitability monotonically decreases as distance increases. Conversely, non-distance-related driving factors (e.g., slope and population density) were standardized using the linear membership function with an S-shaped curve, where suitability gradually decreases as factor values increase. The selection of fuzzy membership functions for driving factors and Boolean values for constraint factors was informed by a comprehensive review of previous studies, as summarized in Table 2.

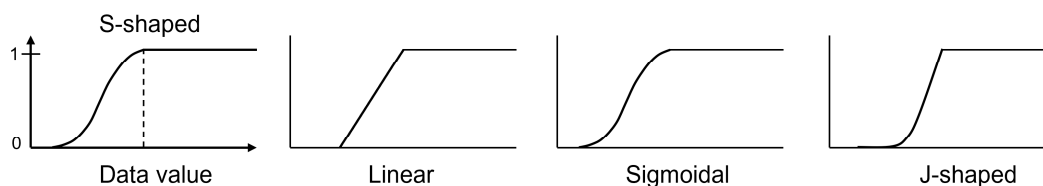


Fig. 3: Types of S-shaped Fuzzy Membership Functions: Linear, Sigmoidal, and J-shaped. Modified from (Bianchini et al., 2019)

Factors	Functions	Influence Distance (meter)
DTM	Linear (S-shaped)	N/A
Slope	Linear (S-shaped)	N/A
Distance to river	Sigmoidal (S-shaped)	150
Flood inundation areas	Linear (S-shaped)	N/A
Population density	Linear (S-shaped)	N/A
Distance to public facilities	Sigmoidal (S-shaped)	150
Distance to roads	Sigmoidal (S-shaped)	100
Distance to residential areas	Sigmoidal (S-shaped)	100
Distance to commercial areas	Sigmoidal (S-shaped)	100
Distance to industrial areas	Sigmoidal (S-shaped)	100
Transportation land	Boolean values (0 or 1)	N/A
Forest land	Boolean values (0 or 1)	N/A
Water bodies	Boolean values (0 or 1)	N/A
Land with a slope greater than 30%	Boolean values (0 or 1)	N/A

Table 2: Standardization of Driving and Constraint Factors Using Fuzzy Membership Functions and Boolean Values.

3.3.7 Multi-Criteria Evaluation (MCE) for Suitability Maps

In the CA-Markov model, MCE integrates multiple driving and constraint factors to generate suitability maps, which indicate the suitability of land use change for a specific land use category at each pixel. The suitability values range from 0 (no suitability) to 255 (highest suitability) for land use change (Lu et al., 2018). MCE encompasses three primary approaches: Weighted Linear Combination (WLC), Boolean Intersection, and Ordered Weighted Average. This study adopts WLC due to its flexibility and ability to incorporate various factors with weighted trade-offs (Eastman, 2015). Accordingly, MCE-WLC was applied to generate suitability maps for all land use types, where WLC is computed using Eq. (4) (Wang & Zheng, 2023):

$$S = \sum w_i x_i \quad (4)$$

where S represents the suitability outcome, w_i denotes the weight assigned to factor i , and x_i is the standardized value of the respective parameter. Furthermore, unlike the Analytic Hierarchy Process (AHP), which relies on expert judgment and may introduce subjectivity, this study employs Cramer's V values to determine the weight of each driving factor in MCE-WLC. Cramer's V quantifies the statistical association between each factor and land use change, ensuring a data-driven and objective weighting approach. Finally, the suitability maps of all land use classes were integrated into the CA model to guide spatial allocation and regulate land use transitions, ensuring that changes occur in areas with higher suitability.

3.3.8 Model Calibration and Validation

To establish the scientific significance of the model in real-world applications and ensure its predictive accuracy, calibration and validation are essential processes (Chakraborty et al., 2022). The Kappa index is a widely used statistical measure for evaluating the agreement between observed and simulated land-use change maps, accounting for chance agreement. The Kappa value typically ranges from 0 to 1, where higher values indicate stronger agreement between predicted and actual data (Aburas et al., 2016; Mitsova et al., 2011; Tong & Feng, 2020). The Kappa coefficient is defined as follows (Pontius, 2000):

$$\text{Kappa} = \frac{(P_o - P_c)}{(P_p - P_c)} \quad (5)$$

where P_o represents the observed proportion of correctly classified data, P_c denotes the expected proportion of agreement by chance, and P_p corresponds to the proportion of perfect agreement. To refine classification accuracy assessments, Pontius (2000) introduced five extended Kappa indices: K_{standard} , K_{histo} , K_{quantity} , K_{location} , and K_{no} . K_{standard} measures overall reliability, K_{histo} evaluates category distribution accuracy, K_{quantity} assesses quantity correctness, K_{location} focuses on spatial accuracy, and K_{no} compares the model's predictive performance against a null model assuming random classification. Furthermore, Kappa values are categorized into five levels: 0.00–0.20 (slight agreement), 0.21–0.40 (fair agreement), 0.41–0.60 (moderate agreement), 0.61–0.80 (substantial agreement), and 0.81–1.00 (almost perfect agreement) (Gwet, 2014; Landis & Koch, 1977; Tong & Feng, 2020). In this study, the VALIDATE module in IDRISI was used to assess the agreement between the observed and simulated 2021 land-use maps, ensuring model calibration. Subsequently, the calibrated model was employed to predict land-use changes for 2035, allowing for an evaluation of the model's long-term predictive performance.

3.4 Flood Modeling with Sobek Model

This study employed the SOBEK model, developed by the Water Resources Agency (MOEA) of Taiwan in collaboration with WL | Delft Hydraulics in the Netherlands, to conduct hydraulic simulations. SOBEK is a comprehensive numerical modeling system widely used for river management, urban drainage, and watershed hydrology analysis. It integrates multiple hydrological and hydraulic components, making it suitable for applications in rural drainage, urban drainage, and river systems. The model features several key hydraulic modules, including the Rainfall-Runoff (RR) module, Channel Flow (CF) module, and Overland Flow (OF) module, enabling both one-dimensional (1D) and two-dimensional (2D) hydrodynamic simulations for flood analysis. To enhance flood modeling accuracy, particularly for overtopping scenarios, this study utilized the Hydraulic Digital Elevation Model (HyDEM), a high-resolution (1-meter) dataset

incorporating overtopping lines, seawalls, and floodgates. Overall, a 1D-2D coupled SOBEK model was applied to simulate flood inundation areas under various rainfall conditions, providing a detailed assessment of flood risks and hydrodynamic behavior.

3.5 Land-Use Strategies for Flood Risk Management

This study first examined the relationship between changes in flood inundation areas and land use transitions following the implementation of flood control engineering measures. The enhancement of flood protection standards may stimulate urban land development. However, given the limitations of flood control infrastructure, overtopping events may still occur, ultimately increasing residual flood risk. Furthermore, residual flood risk is expected to rise with climate change. Spatial planning plays a critical role in flood risk management, particularly through land use planning, which can prevent settlements in high-risk areas, thereby reducing vulnerability. To address this challenge, this study developed six land use management strategies to provide a comprehensive approach to flood risk management and evaluate associated flood risk changes. Previous research has demonstrated that risk-oriented land use planning, such as flood regulation zoning, can effectively mitigate flood risk. Additionally, Low-Impact Development (LID) and Green Infrastructure (GI) measures enhance stormwater storage capacity, reducing surface water accumulation and alleviating flood risk. Therefore, these approaches were selected as land use strategies for evaluating their effectiveness in residual flood risk management. To achieve this, we integrated the CA-Markov model for land use change analysis and the SOBEK model for flood inundation simulation, incorporating hydrological measures such as LID and GI under different rainfall scenarios.

The study considers seven land-use strategy scenarios to evaluate residual flood risk management. Type I (BAU) serves as the baseline, maintaining the existing 6M levee without additional flood control measures. Type II increases the levee height to 10M without land use restrictions, allowing unrestricted development. Type III applies development restrictions in flood-prone areas where inundation exceeds 0.3 meters. Type IV introduces LID measures in flood-prone areas to mitigate surface runoff, while Type V incorporates GI strategies, including permeable water facilities and additional flood retention spaces in parks, green spaces, and agricultural areas. Type VI combines development restrictions (Type III) with GI (Type V) to assess the joint effect of regulatory and green infrastructure strategies. Type VII integrates LID (Type IV) and GI (Type V) to evaluate their combined effectiveness in flood risk reduction. To comprehensively evaluate these scenarios, simulations were conducted under six different rainfall return periods: 10, 25, 50, 100, and 200 years, ranging from normal conditions (10RP or 25RP) to extreme flooding events (200RP). Given the unique characteristics of each scenario, the CA-Markov and SOBEK models were applied accordingly to assess the implications of land use transitions and flood risk changes.

3.6 Flood Risk Assessment Based on Direct Flood Damage Analysis

This study employs direct flood damage analysis to quantify and assess flood risk under different land-use management scenarios. Using the SOBEK 1D-2D hydrodynamic model, we simulated seven land-use strategies under six rainfall return periods (20, 50, 100, 150, and 200 years) within the RCP 6.5 climate change scenario to analyze flood inundation extent and depth. As summarized in Table 3, the assessment focused on residential, commercial, industrial, and agricultural land uses, utilizing flood damage functions derived from previous studies in Taiwan. Direct flood damage was estimated based on flood depth-damage relationships and spatial overlays of land-use maps and flood hazard zones. The study also considered potential land-use transitions and their effects on flood exposure, integrating land-use change projections to evaluate future flood risk under different urban development patterns.

Direct Flood Damage Estimation per 100 m ² (NTD × 10k)				
Flood Depth (m)	Residential	Commercial	Industrial	Agricultural
0.3-1.0	0.21	22.08	16.94	0.03
1.0-2.0	0.31	44.47	45.98	0.03
2.0-3.0	0.38	46.59	53.85	0.03
3.0+	0.43	61.45	75.03	0.03

Table 3: Estimated Direct Flood Damage per 100 m² for Different Land Uses and Flood Depths.

4 RESULTS AND DISCUSSION

4.1 Land Use Change Simulation

4.1.1 Land Use Transition Analysis

This study employed the MC model to analyze land use transitions from 1995 to 2015. As shown in Table 4, the transition areas and probability values were calculated to quantify the likelihood of one land use type converting into another over this period. The results showed a significant increase in industrial, transportation, and commercial land, accompanied by a notable decrease in agricultural and forest land. A closer examination revealed that a large portion of agricultural land was converted into industrial and transportation uses, while much of the forest land was transformed into agricultural, industrial, and transportation areas, likely due to urban growth.

Class	AG	FR	TR	WT	CM	RS	IN	GR	RC	VA	OT
AG	0.2143	0.3112	0.0680	0.0088	0.0151	0.0273	0.0857	0.0063	0.0011	0.0592	0.2030
FR	0.2072	0.5500	0.0462	0.0038	0.0043	0.0160	0.0317	0.0040	0.0021	0.0177	0.1170
TR	0.0331	0.0809	0.4541	0.0182	0.0523	0.1158	0.1095	0.0109	0.0031	0.0720	0.0500
WT	0.0289	0.0370	0.1703	0.2370	0.0084	0.0144	0.0385	0.2683	0.0251	0.0318	0.1404
CM	0.0016	0	0.0692	0	0.1944	0.3871	0.3097	0.0033	0	0.0214	0.0132
RS	0.0411	0.1112	0.1493	0.0072	0.0445	0.4590	0.1078	0.0068	0.0018	0.0308	0.0404
IN	0.0429	0.0335	0.1344	0.0081	0.0856	0.1169	0.4939	0.0101	0.0121	0.0305	0.0320
GR	0	0.1853	0.0309	0	0	0.0772	0	0.4904	0	0	0.2162
RC	0	0	0.1671	0	0	0	0	0.0026	0	0.6214	0.2089
VA	0.2143	0.3112	0.0680	0.0088	0.0151	0.0273	0.0857	0.0063	0.0011	0.0592	0.2030
OT	0.2072	0.5500	0.0462	0.0038	0.0043	0.0160	0.0317	0.0040	0.0021	0.0177	0.1170

Table 4: Land use transition probability based on Markov Chain model from 1995 to 2015.

4.1.2 Driving Factors and Their Influence

Land use changes are driven by environmental, socioeconomic, and built factors, and this study selected relevant factors based on their significance. To evaluate their explanatory power, we employed Cramer's V value, which measures the strength of the correlation between each factor and the observed land-use transitions. This study incorporated flood inundation areas as key factors influencing changes in land use. We utilized flood inundation maps produced by the Water Resources Agency of Taiwan, which cover four rainfall scenarios: 200 mm, 350 mm, 500 mm, and 650 mm within 24 hours.

As shown in the Table 5, the results indicated that the overall Cramer's V values for all selected driving factors exceeded 0.1, demonstrating their significant influence on land use changes. Although the Cramer's V value for flood inundation areas was lower than that of other driving factors, it still exhibited a notable association with land use transitions, likely due to Wugu district's location in a floodplain and previous frequent flooding events. Given the comparative analysis of different rainfall scenarios, we selected the 650mm/24hr scenario as the primary flood inundation factor, as it yielded the highest Cramer's V value.

Environmental Factors	Overall Cramer's V value	Socioeconomic and Built Factors	Overall Cramer's V value
DTM	0.2285	Population density	0.2293
Slope	0.2329	Distance to public facilities	0.2473
Distance to river	0.2004	Distance to roads	0.2184
Flood inundation areas (200mm/24hr)	0.1341	Distance to residential areas	0.2363
Flood inundation areas (350mm/24hr)	0.1351	Distance to commercial areas	0.2625
Flood inundation areas (600mm/24hr)	0.1414	Distance to industrial areas	0.2699
Flood inundation areas (650mm/24hr)	0.1490	N/A	N/A

Table 5: Cramer's V values for all driving factors.

4.1.3 Suitability Mapping Using MCE-WLC

This study first applied fuzzy membership functions to driving factors and Boolean values to constraint factors. The MCE-WLC was employed to generate suitability maps for all land-use types, using Cramer's V as the weighting factor for each variable. As illustrated in Fig. 4, the suitability maps of all 11 land-use types were subsequently integrated with the CA model to enhance the accuracy of future land-use predictions.

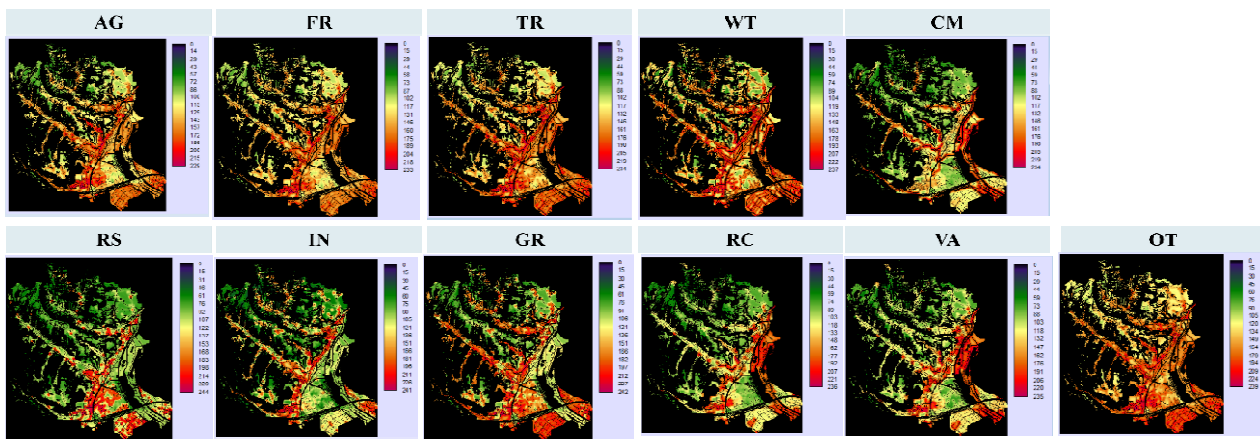


Fig. 4: Suitability Maps for All Land Use Types.

4.1.4 Model Validation and Performance Assessment

The CA-Markov model’s accuracy was assessed using the Kappa coefficient, showing high values ($K_{standard} = 0.7601$, $K_{no} = 0.7958$, $K_{location} = 0.8458$, and $K_{locationStrata} = 0.8458$). Although the values were slightly lower than 80%, they still indicated a moderate to strong agreement between the observed and projected LULC maps. Following validation, the model was deemed suitable for predicting 2035 LULC map.

4.2 Land Use Scenarios and Flood Risk Assessment

4.2.1 Land Use Change under Different Scenarios

This study preliminarily considered two rainfall scenarios, 200 mm and 650 mm over 24 hours, as key driving factors influencing flood-prone areas to analyze the relationship between flood inundation and land use transitions. The 650 mm/24 hr scenario represented extreme flooding, whereas the 200 mm/24 hr scenario reflected reduced flooding. For the preliminary analysis, we utilized flood inundation maps provided by the Water Resources Agency of Taiwan. Additionally, we restricted land use changes in areas where flood depths exceeded 0.3 meters, aligning with land use regulations for flood risk management. As illustrated in Fig. 5, projected 2035 LULC maps under the three scenarios revealed some spatial variations.

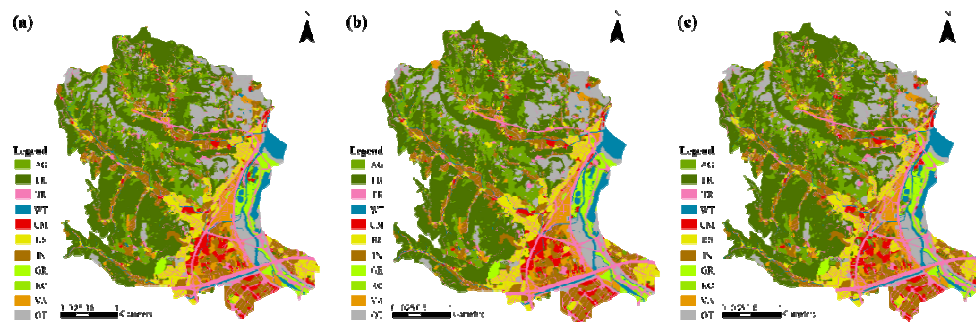


Fig. 5: Projected LULC Maps for 2035 under Different Scenarios: (a) 650mm/24hr, (b) 200mm/24hr, and (c) Restricted Flood Zones.

4.2.2 Impact of Land Use Change on Flood Risk

We overlaid the projected 2035 LULC maps under three scenarios with flood inundation areas for a 650 mm/24-hour rainfall event to compare flood risk. The results showed that under the scenario where 650 mm/24 hours was the key driver, the estimated direct flood damage amounted to 12.4056 billion New Taiwan Dollars (NTD). Under the scenario where 200 mm/24 hours was the key driver, the damage increased to 13.0125 billion NTD. Conversely, when flood-prone areas were effectively restricted, the damage was reduced to 12.0763 billion NTD. The analysis revealed that despite a reduction in flood inundation areas, the flood damage under the 200 mm/24-hour scenario was higher than under extreme rainfall conditions. This phenomenon exemplified the levee effect, where urban expansion accelerated following flood control measures. However, in the absence of effective flood risk management strategies and land use regulations, the overall flood risk still increased. Furthermore, the findings highlighted that controlling flood risk areas was an effective measure to mitigate flood risk. Consistent with previous studies,

these results emphasized the critical role of flood risk-oriented land use planning in ensuring urban resilience, particularly in the face of climate change (Adnan et al., 2020; Pinter et al., 2016).

5 CONCLUSION

This study examined the interplay between the levee effect, residual flood risk, and urban development under climate change, utilizing the CA-Markov model and SOBEK hydrodynamic simulations. The findings reveal that while structural flood control measures, such as reducing flood inundation under normal conditions, they also encouraged land-use changes that inadvertently increase long-term flood risk. The results highlighted the paradox of the levee effect, where enhanced flood protection leads to intensified urban expansion, ultimately exacerbating flood exposure when extreme events exceed design thresholds. The projected land-use scenarios further confirmed that unrestricted urban expansion can elevate direct flood damages despite enhanced flood control infrastructure. Given these insights, policy recommendations emphasize the need for a shift from traditional structural flood control towards a hybrid approach incorporating spatial planning and nature-based solutions. Authorities should implement stricter floodplain development controls, promote sustainable urban design, and enhance public awareness of residual flood risks. Additionally, integrating climate adaptation considerations into land-use policies will be crucial in fostering long-term urban resilience.

6 REFERENCES

- Aburas, M. M., Ho, Y. M., Ramli, M. F., & Ash'aari, Z. H. (2016). The simulation and prediction of spatio-temporal urban growth trends using cellular automata models: A review. *International Journal of Applied Earth Observation and Geoinformation*, 52, 380–389. <https://doi.org/10.1016/j.jag.2016.07.007>
- Adamatzky, A. I. (2018). *Identification Of Cellular Automata*. CRC Press. <https://doi.org/10.1201/9781315274355>
- Adnan, M. S. G., Abdullah, A. Y. M., Dewan, A., & Hall, J. W. (2020). The effects of changing land use and flood hazard on poverty in coastal Bangladesh. *Land Use Policy*, 99, 104868. <https://doi.org/10.1016/j.landusepol.2020.104868>
- Al-sharif, A. A. A., & Pradhan, B. (2014). Monitoring and predicting land use change in Tripoli Metropolitan City using an integrated Markov chain and cellular automata models in GIS. *Arabian Journal of Geosciences*, 7 (10), 4291–4301. <https://doi.org/10.1007/s12517-013-1119-7>
- Bianchini, S., Solari, L., Del Soldato, M., Raspini, F., Montalti, R., Ciampalini, A., & Casagli, N. (2019). Ground Subsidence Susceptibility (GSS) Mapping in Grosseto Plain (Tuscany, Italy) Based on Satellite InSAR Data Using Frequency Ratio and Fuzzy Logic. *Remote Sensing*, 11 (17), Article 17. <https://doi.org/10.3390/rs11172015>
- Breen, M. J., Kebede, A. S., & König, C. S. (2024). Assessing coupled human-flood interactions using LiDAR geostatistics and neighbourhood analyses. *Geomatics, Natural Hazards and Risk*, 15 (1), 2361812. <https://doi.org/10.1080/19475705.2024.2361812>
- Butcher, J. B., Sarkar, S., Johnson, T. E., & Shabani, A. (2023). Spatial analysis of future climate risk to stormwater infrastructure. *JAWRA Journal of the American Water Resources Association*, 59 (6), 1383–1396. <https://doi.org/10.1111/1752-1688.13132>
- Chakraborty, A., Sikder, S., Omrani, H., & Teller, J. (2022). Cellular Automata in Modeling and Predicting Urban Densification: Revisiting the Literature since 1971. *Land*, 11 (7), Article 7. <https://doi.org/10.3390/land11071113>
- D'Angelo, C., Fiori, A., & Volpi, E. (2020). Structural, dynamic and anthropic conditions that trigger the emergence of the levee effect: Insight from a simplified risk-based framework. *Hydrological Sciences Journal*, 65 (6), 914–927. <https://doi.org/10.1080/02626667.2020.1729985>
- Davenport, F., Burke, M., & Diffenbaugh, N. S. (2021). Contribution of historical precipitation change to US flood damages. *PROCEEDINGS OF THE NATIONAL ACADEMY OF SCIENCES OF THE UNITED STATES OF AMERICA*, 118 (4), e2017524118. <https://doi.org/10.1073/pnas.2017524118>
- Dewan, A. M., & Yamaguchi, Y. (2009). Land use and land cover change in Greater Dhaka, Bangladesh: Using remote sensing to promote sustainable urbanization. *Applied Geography*, 29 (3), 390–401. <https://doi.org/10.1016/j.apgeog.2008.12.005>
- Di Baldassarre, G., Kreibich, H., Vorogushyn, S., Aerts, J., Arnbjerg-Nielsen, K., Barendrecht, M., Bates, P., Borga, M., Botzen, W., Bubeck, P., De Marchi, B., Llasat, C., Mazzoleni, M., Molinari, D., Mondino, E., Mård, J., Petrucci, O., Scolobig, A., Viglione, A., & Ward, P. J. (2018). Hess Opinions: An interdisciplinary research agenda to explore the unintended consequences of structural flood protection. *Hydrology and Earth System Sciences*, 22 (11), 5629–5637. <https://doi.org/10.5194/hess-22-5629-2018>
- Ding, M., Lin, P., Gao, S., Wang, J., Zeng, Z., Zheng, K., Zhou, X., Yamazaki, D., Gao, Y., & Liu, Y. (2023). Reversal of the levee effect towards sustainable floodplain management. *Nature Sustainability*, 6 (12), 1578–1586. <https://doi.org/10.1038/s41893-023-01202-9>
- Eastman, J. R. (2015). *TerrSet manual*. Accessed in TerrSet Version, 18 (1).
- Ferdous, M. R., Wesselink, A., Brandimarte, L., Di Baldassarre, G., & Rahman, M. M. (2019). The levee effect along the Jamuna River in Bangladesh. *Water International*, 44 (5), 496–519. Scopus. <https://doi.org/10.1080/02508060.2019.1619048>
- Fusinato, E., Han, S., Kobiyama, M., & de Brito, M. M. (2024). Safe development paradox: Evidence and methodological insights from a systematic review. *Natural Hazards*. <https://doi.org/10.1007/s11069-024-06774-z>
- Gwet, K. L. (2014). *Handbook of Inter-Rater Reliability*, 4th Edition: The Definitive Guide to Measuring The Extent of Agreement Among Raters. Advanced Analytics, LLC.

- Islam, K., Rahman, Md. F., & Jashimuddin, M. (2018). Modeling land use change using Cellular Automata and Artificial Neural Network: The case of Chunati Wildlife Sanctuary, Bangladesh. *Ecological Indicators*, 88, 439–453. <https://doi.org/10.1016/j.ecolind.2018.01.047>
- Jokar Arsanjani, J., Helbich, M., Kainz, W., & Darvishi Bolorani, A. (2013). Integration of logistic regression, Markov chain and cellular automata models to simulate urban expansion. *International Journal of Applied Earth Observation and Geoinformation*, 21, 265–275. <https://doi.org/10.1016/j.jag.2011.12.014>
- Kim, J., Porter, J., & Kearns, E. J. (2023). Exposure of the US population to extreme precipitation risk has increased due to climate change. *Scientific Reports*, 13 (1), 21782. <https://doi.org/10.1038/s41598-023-48969-7>
- Landis, J. R., & Koch, G. G. (1977). The Measurement of Observer Agreement for Categorical Data. *Biometrics*, 33 (1), 159–174. <https://doi.org/10.2307/2529310>
- Li, J., Zeng, J., Huang, G., & Chen, W. (2024). Urban Flood Mitigation Strategies with Coupled Gray–Green Measures: A Case Study in Guangzhou City, China. *International Journal of Disaster Risk Science*, 15 (3), 467–479. <https://doi.org/10.1007/s13753-024-00566-6>
- Liu, Y., & Feng, Y. (2012). A Logistic Based Cellular Automata Model for Continuous Urban Growth Simulation: A Case Study of the Gold Coast City, Australia. In A. J. Heppenstall, A. T. Crooks, L. M. See, & M. Batty (Eds.), *Agent-Based Models of Geographical Systems* (pp. 643–662). Springer Netherlands. https://doi.org/10.1007/978-90-481-8927-4_32
- Lu, Q., Chang, N.-B., Joyce, J., Chen, A. S., Savic, D. A., Djordjevic, S., & Fu, G. (2018). Exploring the potential climate change impact on urban growth in London by a cellular automata-based Markov chain model. *Computers, Environment and Urban Systems*, 68, 121–132. <https://doi.org/10.1016/j.compenvurbsys.2017.11.006>
- Ludy, J., & Kondolf, G. M. (2012). Flood risk perception in lands “protected” by 100-year levees. *NATURAL HAZARDS*, 61 (2), 829–842. <https://doi.org/10.1007/s11069-011-0072-6>
- Merz, B., Blöschl, G., Vorogushyn, S., Dottori, F., Aerts, J. C. J. H., Bates, P., Bertola, M., Kemter, M., Kreibich, H., Lall, U., & Macdonald, E. (2021). Causes, impacts and patterns of disastrous river floods. *Nature Reviews Earth & Environment*, 2 (9), 592–609. <https://doi.org/10.1038/s43017-021-00195-3>
- Mitsova, D., Shuster, W., & Wang, X. (2011). A cellular automata model of land cover change to integrate urban growth with open space conservation. *Landscape and Urban Planning*, 99 (2), 141–153. <https://doi.org/10.1016/j.landurbplan.2010.10.001>
- Moghadam, H. S., & Helbich, M. (2013). Spatiotemporal urbanization processes in the megacity of Mumbai, India: A Markov chains-cellular automata urban growth model. *APPLIED GEOGRAPHY*, 40, 140–149. <https://doi.org/10.1016/j.apgeog.2013.01.009>
- O’Donnell, E. C., & Thorne, C. R. (2020). Drivers of future urban flood risk. *Philosophical Transactions of the Royal Society A: Mathematical, Physical and Engineering Sciences*, 378 (2168), 20190216. <https://doi.org/10.1098/rsta.2019.0216>
- Pinter, N., Huthoff, F., Dierauer, J., Remo, J. W. F., & Dampitz, A. (2016). Modeling residual flood risk behind levees, Upper Mississippi River, USA. *Environmental Science & Policy*, 58, 131–140. <https://doi.org/10.1016/j.envsci.2016.01.003>
- Pontius, R. G. (2000). Quantification error versus location error in comparison of categorical maps. *PHOTOGRAMMETRIC ENGINEERING AND REMOTE SENSING*, 66 (8), 1011–1016.
- Roberto, R., Barontini, S., & Ferri, M. (2015). Structural Residual Risk Due to Levee Failures in Flood Mapping. In G. Lollino, M. Arattano, M. Rinaldi, O. Giustolisi, J.-C. Marechal, & G. E. Grant (Eds.), *Engineering Geology for Society and Territory – Volume 3* (pp. 449–452). Springer International Publishing. https://doi.org/10.1007/978-3-319-09054-2_92
- Sang, L., Zhang, C., Yang, J., Zhu, D., & Yun, W. (2011). Simulation of land use spatial pattern of towns and villages based on CA–Markov model. *Mathematical and Computer Modelling*, 54 (3), 938–943. <https://doi.org/10.1016/j.mcm.2010.11.019>
- Serra-Llobet, A., Tourment, R., Montané, A., & Buffin-Belanger, T. (2022). Managing residual flood risk behind levees: Comparing USA, France, and Quebec (Canada). *Journal of Flood Risk Management*, 15 (2), e12785. <https://doi.org/10.1111/jfr3.12785>
- Sisay, G., Gessesse, B., Fürst, C., Kassie, M., & Kebede, B. (2023). Modeling of land use/land cover dynamics using artificial neural network and cellular automata Markov chain algorithms in Goang watershed, Ethiopia. *Heliyon*, 9 (9), e20088. <https://doi.org/10.1016/j.heliyon.2023.e20088>
- Tan, X., Deng, M., Chen, K., Shi, Y., Zhao, B., & Liu, Q. (2024). A spatial hierarchical learning module based cellular automata model for simulating urban expansion: Case studies of three Chinese urban areas. *GISCIENCE & REMOTE SENSING*, 61 (1), 2290352. <https://doi.org/10.1080/15481603.2023.2290352>
- Tanoue, M., Taguchi, R., Alifu, H., & Hirabayashi, Y. (2021). Residual flood damage under intensive adaptation. *Nature Climate Change*, 11 (10), Article 10. <https://doi.org/10.1038/s41558-021-01158-8>
- Tong, X., & Feng, Y. (2020). A review of assessment methods for cellular automata models of land-use change and urban growth. *International Journal of Geographical Information Science*, 34 (5), 866–898. <https://doi.org/10.1080/13658816.2019.1684499>
- Wang, L., Cui, S., Li, Y., Huang, H., Manandhar, B., Nitivattananon, V., Fang, X., & Huang, W. (2022). A review of the flood management: From flood control to flood resilience. *Heliyon*, 8 (11), e11763. <https://doi.org/10.1016/j.heliyon.2022.e11763>
- Wang, S., & Zheng, X. (2023). Dominant transition probability: Combining CA–Markov model to simulate land use change. *Environment, Development and Sustainability*, 25 (7), 6829–6847. <https://doi.org/10.1007/s10668-022-02337-z>
- White, G. F. (1958). *Changes in Urban Occupance of Flood Plains in the United States*. University of Chicago.
- White, G. F., Kates, R. W., & Burton, I. (2001). Knowing better and losing even more: The use of knowledge in hazards management. *Global Environmental Change Part B: Environmental Hazards*, 3 (3), 81–92. [https://doi.org/10.1016/S1464-2867\(01\)00021-3](https://doi.org/10.1016/S1464-2867(01)00021-3)